Kinetic theory of resistive ballooning modes

P. H. Diamond, P. L. Similon, T. C. Hender, and B. A. Carreras

Citation: The Physics of Fluids **28**, 1116 (1985);
View online: https://doi.org/10.1063/1.865406
View Table of Contents: http://aip.scitation.org/toc/pfl/28/4
Published by the American Institute of Physics

Kinetic theory of resistive ballooning modes

P. H. Diamond and P. L. Similon
Institute for Fusion Studies, Austin, Texas 78712

T. C. Hender and B. A. Carreras
Oak Ridge National Laboratory, P. O. Box Y, Oak Ridge, Tennessee 37831

(Received 7 November 1983; accepted 2 December 1984)

A linear and nonlinear kinetic theory of resistive ballooning modes that includes diamagnetic drifts and finite Larmor radius effects is presented. The linear stability of resistive ballooning modes is examined analytically and numerically. A renormalized resistive ballooning equation is derived, and the saturation level of the instabilities is analytically calculated. Finally, a calculation of the electron thermal conductivity for the large ω_* regime is presented.

I. INTRODUCTION

The stability properties of resistive ballooning modes[1] have been extensively studied using the magnetohydrodynamic (MHD) equations.[2–4] Recently, resistive ballooning mode turbulence has been advanced as a possible explanation for the confinement degradation at high poloidal beta (β_p) observed in the Impurity Study Experiment (ISX-B) tokamak.[5] The reduced resistive MHD model, where pressure evolves by fluid convection, predicts unstable resistive ballooning modes with a growth rate $\gamma \sim \eta^{1/3}\beta_p^{2/3}$. Numerical calculations indicate that a simple mixing length theory adequately describes nonlinear saturation.[5] These results are then used to calculate the stochastic magnetic field diffusion coefficient D_M and the anomalous electron thermal conductivity χ_e. The theoretical prediction of χ_e correlates well with experimental observation.[5]

In order to fully understand, develop, and broaden the domain of applicability of the theory, several questions and issues must be addressed. In a recent paper[6] the linear stability of resistive ballooning modes was studied using the full MHD model. For discharges with high β_p, low current, and relatively low electron temperature, the predictions of the full MHD model are in good agreement with those of the pressure convection model. For high current and high-temperature plasmas, compressibility has a strong stabilizing effect, as described in Ref. 2. In a future publication, the theory of nonlinear saturation and the calculation of χ_e will be discussed in detail.

In this paper the linear and nonlinear kinetic theory of resistive ballooning modes is presented as an extension of the work presented in Refs. 5 and 6. Several specific questions are addressed. These include:

(1) How does the inclusion of kinetic effects associated with finite Larmor radius, diamagnetic frequency, and drift frequency modify the basic structure and linear stability of resistive ballooning modes?

(2) How is a nonlinear theory of kinetic resistive ballooning modes constructed? What are the principal nonlinear effects? What is the effect of finite ω_*?

(3) How do kinetic effects modify the calculation of χ_e? Is χ_e necessarily reduced in proportion to the reduction in linear growth rate?

Here these questions are addressed and answered for the parameter regime relevant to resistive plasmas such as those occurring in ISX-B. A detailed kinetic theory of resistive ballooning modes is developed from the basic gyrokinetic equations. The linear stability is examined analytically and numerically. While finite ω_* and Larmor radius reduce the growth rates, instability persists throughout the parameter regime of interest. It is shown analytically that purely growing modes can occur. A renormalized resistive ballooning equation is derived from the renormalized kinetic equations. The basic structure, properties, and constraints imposed on the nonlinear theory are discussed. A comparison with the more familiar kinetic theories of drift wave turbulence is made. The principal nonlinear effects, associated with diffusion of ion density, electron and ion pressure, and electron parallel pressure, nonlinearly modify the inertia, curvature drive, and Ohm's law terms, respectively. Finite ω_* can introduce nonlinear frequency shifts. Finally, χ_e is calculated for the large ω_* regime. It is shown that while kinetic corrections reduce the growth rate, they can also increase the size of magnetic perturbations relative to the electrostatic perturbations. These two effects tend to partially offset each other in their modifications to χ_e.

The remainder of this paper is organized in the following fashion. In Sec. II the linear kinetic resistive ballooning equations are derived from the gyrokinetic equations. In Secs. III and IV the analytical and numerical predictions of linear stability are presented and discussed. In Sec. V the nonlinear kinetic theory is presented and χ_e is calculated for the large ω_* regime.

II. DERIVATION OF THE RESISTIVE BALLOONING EIGENMODE EQUATIONS

In this section the moment equations that describe resistive ballooning instabilities are derived from the electron and ion gyrokinetic equations. The assumption of short electron mean-free-path, $\lambda_{\rm mfp} < Rq$, is made throughout. Here R is the distance to the axis of the torus and q the safety factor. The effects of finite electron and ion diamagnetic frequency, finite ion gyroradius, and finite ion and electron magnetic drift (compression) are retained. The results obtained from the kinetic theory reduce smoothly to those obtained previously, using the resistive MHD model.[6]

The low-frequency gyrokinetic equation that describes electromagnetic fluctuations in toroidal geometry[7–9] is

$$-i(\omega-\omega_{Ds})\,g_n^s+\frac{V_\parallel^s}{Rq}\frac{\partial g_n^s}{\partial y}+\mathscr{C}(s,s')\,g_n^s$$

 0031-9171/85/041116-10$01.90

$$= -\frac{iq_s}{T_s}(\omega - \omega_{*s})\langle f^s\rangle J_0(k_\perp \rho^s)\left(\Phi_n - \frac{V_\parallel^s}{c}A_{\parallel n}\right), \tag{1}$$

where

$$n_n^s = -\frac{q_s}{T_s}\Phi_n + \int d^3V^s g_n^s J_0(k_\perp \rho^s). \tag{2}$$

Here g_n^s, $\langle f_s\rangle$, and n_n^s are the nonadiabatic perturbed distribution function, the averaged distribution function, and the density fluctuation of species s ($s = e,i$), respectively. The subindex n indicates the toroidal mode number n. The functions Φ_n and $A_{\parallel n}$ are the electrostatic potential fluctuation and the parallel component of the vector potential fluctuation. Because $\beta \ll 1$ (though the case $\beta_p \gtrsim 1$ is considered here), the effects of coupling to compressional Alfvén waves, associated with the parallel magnetic field fluctuations, are neglected. The extended poloidal coordinate is denoted by y, and ω is the mode frequency. The diamagnetic drift frequency is $\omega_{*s} = -k_\theta a_s V_s/L_n$, where $k_\theta = nq/\rho$, $L_n^{-1} = -d\ln(n_e)/d\rho$, $V_s = (T_s/m_i)^{1/2}$, and $a_s = cm_iV_s/(q_sB_0)$. The charge and mass of the species s are q_s and m_s, respectively, and the equilibrium temperature and density are T_s and n_s. $\mathscr{C}$ is a number conserving collision operator for like-species ($s - s$) and interspecies (s – s') collisions. The effects of temperature gradients are neglected but may be easily inserted. The Bessel function $J_0(k_\perp \rho^s)$ results from the average over gyro-orbits. Here ρ^s is the gyroradius of species s. The magnetic curvature drift frequency is

$$\omega_{Ds} = \epsilon_T \omega_{*s}\frac{(V_\parallel^s)^2 + \frac{1}{2}(V_\perp^s)^2}{2T_s/m_i}\hat{K}(y), \tag{3}$$

where $\epsilon_T = L_n/R$ and

$$\hat{K}(y) = (2R/k_\theta B_0^2)(\mathbf{B}_0\times\nabla B_0)\cdot\mathbf{k}_\perp \tag{4}$$

is the toroidal curvature term, with contributions of order beta neglected; $\mathbf{B}_0 = I\nabla\zeta + \nabla\zeta\times\nabla\psi$ is the equilibrium magnetic field; and $k_\perp^2 = n^2\alpha(\rho,y)$, where in the straight field line coordinate system (ρ,θ,ζ) used in Ref. 6,

$$\alpha(\rho,y) = 1/R^2 + (q^2/\rho^2)(\hat{S}^2y^2g^{\rho\rho} + 2\hat{S}yg^{\rho\theta} + g^{\theta\theta}), \tag{5}$$

$\hat{S} = \rho(dq/d\rho)/q$ being the shear parameter. In this coordinate system, the toroidal curvature term $\hat{K}$ can be written as

$$\hat{K}(y) = -2\frac{RR_0}{I}\left[\frac{\partial B_0}{\partial\rho} + \frac{I^2}{R^2B_0^2}\times\left(\frac{\rho g^{\rho\theta}}{q^2R_0^2} - \frac{y}{q}\frac{dq}{d\rho}\right)\frac{\partial B_0}{\partial y}\right]. \tag{6}$$

Two macroscopic equations are required in order to describe resistive ballooning modes. The first is constructed by subtracting the $V_\parallel$ moment of the electron kinetic equation from that of the ion kinetic equation. This yields

$$\frac{i}{\omega}\frac{a_e^2V_A^2}{c^2}\frac{1}{Rq}\frac{\partial J_{\parallel n}}{\partial y} = \tau\left(1 - \frac{\omega_{*i}}{\omega}\right)[\Gamma_0(b_i) - 1]\Phi_n + \frac{T_e}{|e|}\left(\int d^3V^i\frac{\omega_{Di}}{\omega}J_0(k_\perp\rho^i)g_n^i - \int d^3V^e\frac{\omega_{De}}{\omega}g_n^e\right), \tag{7}$$

where $J_{\parallel n}$ is the parallel current density perturbation, $b_i = (k_\perp\rho^i)^2$, and it is assumed that $k_\perp^2(\rho^e)^2 \to 0$. Here $\tau = T_e/T_i$ is the temperature ratio, and $V_A^2 = B_0^2/n_im_i$ is the square of the Alfvén velocity. The quasineutrality condition has been used to eliminate the nonadiabatic density perturbations. Notice that Eq. (7) is equivalent to the condition that $\nabla\cdot\mathbf{J} = 0$, where the left-hand side accounts for $\nabla_\parallel J_\parallel$ because of field line bending and the right-hand side accounts for the contributions to $\nabla_\perp\cdot\mathbf{J}_\perp$ from inertia (polarization drift) and curvature drift.

The curvature drift terms in Eq. (7), which include the destabilizing pressure effects, are calculated by obtaining g_n^e and g_n^i from the solution of Eq. (1). The nonadiabatic electron response g_n^e may be obtained in the case of interest ($|\mathscr{C}(s,s')| > \omega_{Te}$ and $\omega > \omega_{De}$, where ω_{Ts} is the transit frequency of species s) by noting that to lowest order,

$$\mathscr{C}g_n^{e(0)} = 0 \tag{8}$$

implies

$$g_n^{e(0)} = f_0(\mathbf{V}^e)\bar{g}_n^e(y), \tag{9}$$

where $f_0(\mathbf{V}^e)$ can, in general, be a shifted Maxwellian. Here the approximation $f_0(\mathbf{V}^e) = \langle f^e\rangle$ is sufficient. To first order, Eq. (1) then becomes

$$-i(\omega - \omega_{De})\langle f^e\rangle\bar{g}_n^e + \frac{V_\parallel^e}{Rq}\frac{\partial}{\partial y}(\langle f^e\rangle\bar{g}_n^e) + \mathscr{C}g_n^{e(1)} = (i|e|/T_e)(\omega - \omega_{*e})\langle f^e\rangle[\Phi_n - (V_\parallel/c)A_{\parallel n}]. \tag{10}$$

Integrating Eq. (10) over velocity, noting $\mathscr{C}$ is number conserving, and taking $\langle f^e\rangle$ to be even in velocity, the nonadiabatic electron response

$$g_n^e = -\frac{|e|}{T_e}\frac{\omega - \omega_{*e}}{\omega - \bar{\omega}_{De}}\langle f^e\rangle\Phi_n \tag{11}$$

is obtained, where for $\omega > \bar{\omega}_{De} \equiv \int d^3V\langle f^e\rangle\omega_{De}$,

$$g_n^e \cong -\frac{|e|}{T_e}\left(1 - \frac{\omega_{*e}}{\omega}\right)\left(1 + \frac{\bar{\omega}_{De}}{\omega}\right)\langle f^e\rangle\Phi_n. \tag{12}$$

Similarly, for $\omega > \omega_{Ti}$ and $\omega > \omega_{Di}, C_{ie}, C_{ii}$, the nonadiabatic ion response g_n^i is

$$g_n^i = \frac{|e|}{T_i}\frac{\omega - \omega_{*i}}{\omega - \omega_{Di}}\langle f^i\rangle\Phi_n J_0(k_\perp\rho^i) \tag{13}$$

and, for $\omega > \omega_{Di}$,

$$g_n^i \cong \frac{|e|}{T_i}\left(1 - \frac{\omega_{*i}}{\omega}\right)\left(1 + \frac{\omega_{Di}}{\omega}\right)\langle f^i\rangle J_0(k_\perp\rho^i)\Phi_n. \tag{14}$$

The $V_\parallel A_{\parallel n}/c$ contribution to g_n^i has been omitted, anticipating later velocity integrations. For modes that survive stabilization by perpendicular compression, the requirement that mode frequency exceed the ion transit frequency $\omega > \omega_{T_i}$ is automatically satisfied[6] for $T_i \approx T_e$. Finally, the effects of ion drift resonance are not considered here.

Substituting Eqs. (12) and (14) into Eq. (7) gives

$$\frac{i}{\omega}\frac{a_e^2V_A^2}{c^2}\frac{1}{Rq}\frac{\partial J_{\parallel n}}{\partial y} = \tau\left(1 - \frac{\omega_{*i}}{\omega}\right)[\Gamma_0(b_i) - 1]\Phi_n + \left[\tau\left(1 - \frac{\omega_{*i}}{\omega}\right)\int d^3V^i\frac{\omega_{Di}}{\omega}\right.$$

$$\times\left(1+\frac{\omega_{Di}}{\omega}\right)J_0^2(k_\perp\rho^i)\langle f^i\rangle$$
$$+\left(1-\frac{\omega_{*e}}{\omega}\right)\frac{\overline{\omega}_{De}}{\omega}\left(1+\frac{\overline{\omega}_{De}}{\omega}\right)\Bigg]\Phi_n, \tag{15}$$

which for $b_i<1$, and ignoring perpendicular compressibility yields

$$\frac{i}{\omega}\frac{a_e^2V_A^2}{c^2}\frac{1}{Rq}\frac{\partial J_{\|n}}{\partial y}$$
$$=-\left(1-\frac{\omega_{*i}}{\omega}\right)k_\perp^2a_e^2\Phi_n$$
$$-k_\theta^2a_e^2\left[\left(1+\frac{T_e}{T_e}\right)\frac{\gamma_I^2}{\omega^2}\hat{K}(y)\right.$$
$$\left.+\frac{T_i}{T_e}\left(1-\frac{\omega_{*i}}{\omega}\right)\frac{\overline{\omega}_{Di}}{\omega}\frac{\rho^2}{q^2}\alpha(\rho,y)\right]\Phi_n; \tag{16}$$

here $\gamma_I^2=\epsilon_TV_e^2/L_n^2$. With these approximations two terms result from the curvature drift contribution. The first is the usual ballooning driving term of standard magnetohydrodynamics and the second reflects charge separation caused by finite ion gyroradius. In the limit $T_i/T_e\to0$, $\omega_{*i}/\omega\to0$, Eq. (16) reduces to the perpendicular momentum balance equation of magnetohydrodynamics, with the pressure evolving by fluid convection.

The second macroscopic equation is constructed by taking the $V_\|$ moment of the electron kinetic equation and using the result of Eq. (12) to compute the parallel pressure and thus close the moment hierarchy. The resulting equations in the limit $\nu>\omega,\overline{\omega}_{De}$ are

$$\nu_{ei}J_{\|n}+\frac{1}{Rq}\frac{\partial P_{\|n}}{\partial y}=\frac{i\omega_{pe}^2}{4\pi}(\omega-\omega_{*e})\frac{A_{\|n}}{c}, \tag{17}$$

$$P_{\|n}=-\frac{\omega_{pe}^2}{4\pi}\left(1-\frac{\omega_{*e}}{\omega}\right)\left(1+\frac{\overline{\omega}_{De}}{\omega}\right)\Phi_n, \tag{18}$$

where ν_{ei} is the electron–ion collision frequency and ω_{pe} is the electron-plasma frequency, $\omega_{pe}^2=4\pi n_e|e|^2/m_e$. These equations relate the parallel current $J_{\|n}\approx J_\|^e$ to Φ_n and $A_{\|n}$ and constitute a finite diamagnetic frequency modified Ohm's law. Substituting Eq. (18) into Eq. (17) yields

$$\nu_{ei}J_{\|n}=\frac{\omega_{pe}^2}{4\pi}\left(1-\frac{\omega_{*e}}{\omega}\right)\left[E_{\|n}+\frac{1}{qR}\frac{d}{dy}\left(\frac{\omega_{De}}{\omega}\phi_n\right)\right], \tag{19}$$

where

$$E_{\|n}=i\frac{\omega}{c}A_{\|n}+\frac{1}{Rq}\frac{\partial\Phi_n}{\partial y}. \tag{20}$$

Note that in the limit $\omega_{*e}/\omega\to0$, Eq. (18) reduces to Ohm's law of resistive magnetohydrodynamics.

Using the parallel component of Ampére's law, Eqs. (16) and (19) can be combined to obtain a single second-order ballooning equation for Φ_n:

$$\frac{\partial}{\partial y}\left[\frac{(1-\omega_{*e}/\omega)(\rho^2/q^2)\alpha(\rho,y)}{1-\omega_{*e}/\omega+i\eta(k_\perp^2/\omega)}\left(1+\frac{\overline{\omega}_{De}}{\omega}\right)\frac{\partial\Phi_n}{\partial y}\right]$$
$$+\left(1-\frac{\omega_{*i}}{\omega}\right)\frac{\omega^2}{\omega_A^2}\frac{\rho^2}{q^2}\alpha\Phi_n+\left[\left(1+\frac{T_i}{T_e}\right)\frac{\gamma_I^2}{\omega_A^2}\hat{K}(y)\right.$$
$$\left.+\frac{T_i}{T_e}\left(1-\frac{\omega_{*i}}{\omega}\right)\frac{\omega\overline{\omega}_{Di}}{\omega_A^2}\frac{\rho^2}{q^2}\alpha\right]\Phi_n=0, \tag{21}$$

with $\omega_A=V_A/Rq$ and $\eta=4\pi\nu_{ei}c^2/\omega_{pe}^2$. Equation (21) is the eigenmode equation for resistive ballooning modes and incorporates the effects of finite $\omega_{*e},\omega_{*i},T_i/T_e$ [equivalent to $k_\perp^2(\rho^i)^2$]. In the limit $\omega_{*e}/\omega\to0$, $\omega_{*i}/\omega\to0$, $T_i/T_e\to0$, Eq. (21) reduces to the resistive ballooning equation of magnetohydrodynamics, where pressure evolution is described by convection.[6] Equation (21) may be simplified by using a shifted circle approximation to the equilibrium,

$$\hat{K}(y)=2(D_0+\cos y+\hat{S}y\sin y), \tag{22}$$

$$\alpha(\rho,y)=(q^2/\rho^2)[1+\hat{S}^2y^2+2D_0(\cos y+\hat{S}y\sin y)]. \tag{23}$$

From Eq. (21) it then follows that

$$\frac{\partial}{\partial y}\left[\frac{(1-\omega_{*e}/\omega)(1+\hat{S}^2y^2)}{1-\omega_{*e}/\omega+i(\eta k_\perp^2/\omega)}\left(1+\frac{\overline{\omega}_{De}}{\omega}\right)\frac{\partial\Phi_n}{\partial y}\right]$$
$$+\left(1-\frac{\omega_{*i}}{\omega}\right)\frac{\omega^2}{\omega_A^2}(1+\hat{S}^2y^2)\Phi_n$$
$$+\left[\left(1+\frac{T_i}{T_e}\right)\frac{\gamma_I^2}{\omega_A^2}\hat{K}(y)\right.$$
$$\left.+\frac{T_i}{T_e}\left(1-\frac{\omega_{*i}}{\omega}\right)\frac{\omega\overline{\omega}_{Di}}{\omega_A^2}(1+\hat{S}^2y^2)\right]\Phi_n=0, \tag{24}$$

where the average curvature D_0 has been ignored.

Equation (24) may be further simplified by noting that for $\omega_{*i}\gg\omega$,

$$\frac{T_i}{T_e}\left(1-\frac{\omega_{*i}}{\omega}\right)\frac{\omega\overline{\omega}_{Di}}{\omega_A^2}(1+\hat{S}^2y^2)$$
$$\cong-\frac{T_i}{T_e}\frac{\gamma_I^2}{\omega_A^2}\hat{K}(y)k_\perp^2(\rho^i)^2, \tag{25}$$

and for $\omega_{*i}<\omega$,

$$\frac{T_i}{T_e}\left(1-\frac{\omega_{*i}}{\omega}\right)\frac{\omega\overline{\omega}_{Di}}{\omega_A^2}(1+\hat{S}^2y^2)$$
$$\cong\frac{T_i}{T_e}\frac{\overline{\omega}_{Di}\omega}{\omega_A^2}(1+\hat{S}^2y^2). \tag{26}$$

As $k_\perp^2(\rho^i)^2<1$, and for $(\overline{\omega}_{Di}/\omega)(1+\hat{S}^2y^2)<1$, Eq. (24) becomes

$$\frac{\partial}{\partial y}\left[\frac{(1-\omega_{*e}/\omega)(1+\hat{S}^2y^2)}{1-\omega_{*e}/\omega+i\eta k_\perp^2/\omega}\left(1+\frac{\overline{\omega}_{De}}{\omega}\right)\frac{\partial\Phi_n}{\partial y}\right]$$
$$+\left(1-\frac{\omega_{*i}}{\omega}\right)\frac{\omega^2}{\omega_A^2}(1+\hat{S}^2y^2)\Phi_n$$
$$+\left(1+\frac{T_i}{T_e}\right)\frac{\gamma_I^2}{\omega_A^2}\hat{K}(y)\Phi_n=0. \tag{27}$$

Note that $(1+\hat{S}^2y^2)<\omega/\overline{\omega}_{Di}$ is consistent with the constraint on poloidal mode extent imposed by the criterion for resistive MHD instability $\gamma>\omega_c\equiv V_e(1+T_i/T_e)^{1/2}/R$, which was derived in Ref. 6.

It is important to note that the derivation presented here is valid only when $k_\perp^2a_e^2<1$ and when the mode frequency ω is larger than ω_D,ω_{Ti}, and ω_c. The first restriction ensures that for $\omega_*>\omega$ the effects of ion polarization drift are small and, hence, that density evolves primarily by con-

vection ($\omega_* / \omega > k_\perp^2 a_e^2$). It then follows from Eq. (6) and the second restriction that the $\nabla_\parallel J_\parallel$ contributions to density evolution, which appear in the reduced Braginskii model,[10,11] are also small. Finally, $\omega > \omega_{Ti}$ is necessary for hydrodynamic ion response. In adiabatic ion regimes ($\omega < \omega_{Ti}$), the resistive ballooning mode is stabilized.

III. APPROXIMATE ANALYTIC SOLUTION

In this section an approximate analytical solution to the simplified kinetic resistive ballooning equation [Eq. (25)] is presented. Following Ref. 6, a two-scale expansion procedure is used to solve Eq. (25). Thus, Φ_n is written as

$$\Phi_n = \bar{\Phi}_n(y) + \tilde{\Phi}_n(y)(\cos y + \hat{S} y \sin y), \tag{28}$$

where $\bar{\Phi}_n(y)$ and $\tilde{\Phi}_n(y)$ are slowly varying coefficients relative to the fast fluctuations of scale length 2π. Ignoring the weak effects of average curvature, it follows that the envelope equation for $\bar{\Phi}_n(y)$ is

$$\frac{\partial}{\partial y}\left(\frac{(\omega-\omega_{*e})(1+\hat{S}^2y^2)}{\omega-\omega_{*e}+i\eta k_\perp^2}\frac{\partial\bar{\Phi}_n}{\partial y}\right)+(1+\hat{S}^2y^2)\left\{\frac{\omega(\omega-\omega_{*i})}{\omega_A^2}+\left[\left(\frac{\omega-\omega_{*e}}{\omega-\omega_{*e}+i\eta k_\perp^2}-\frac{\omega(\omega-\omega_{*i})}{\omega_A^2}\right)(1+\hat{S}^2y^2)\right]^{-1}\times\left(1+\frac{T_i}{T_e}\right)^2\frac{2\gamma_I^4}{\omega_A^4}\right\}\bar{\Phi}_n=0. \tag{29}$$

The curvature drift correction to the field line bending term oscillates rapidly at large y, where the field and fluid decouple. Hence it makes little contribution to the field line bending and is ignored hereafter.

At large values of y, where the field line bending is weakened by resistive dissipation, $\eta k_\perp^2 > |\omega - \omega_{*e}|$. In that case, the electrostatic approximation is applicable, and Eq. (29) reduces to

$$\frac{\partial}{\partial y}\left(\frac{(\omega-\omega_{*e})(1+\hat{S}^2y^2)}{\omega-\omega_{*e}+i\eta k_\perp^2}\frac{\partial\bar{\Phi}_n}{\partial y}\right)+(1+\hat{S}^2y^2)\left[\frac{\omega(\omega-\omega_{*i})}{\omega_A^2}+i\frac{2\eta k_\theta^2}{\omega-\omega_{*e}}\left(1+\frac{T_i}{T_e}\right)^2\frac{\gamma_I^2}{\omega_A^4}\right]\bar{\Phi}_n=0. \tag{30}$$

Equating the coefficient of $(1+\hat{S}^2y^2)$ to zero yields the dispersion relation

$$(\omega-\omega_{*i})\omega+\frac{2i\eta k_\theta^2}{\omega-\omega_{*e}}\left(1+\frac{T_i}{T_e}\right)^2\frac{\gamma_I^4}{\omega_A^2}=0. \tag{31}$$

or, with $\omega = i\gamma$,

$$\gamma(\gamma+i\omega_{*i})(\gamma+i\omega_{*e})=\gamma_0^3. \tag{32}$$

Here $\gamma_0^3 = 2\eta k_\theta^2 n_i^2(T_e+T_i)^2q^2/[(B_0L_n)^2m_i n_i]$, where γ_0 is the linear growth rate as given by resistive magnetohydrodynamics, with pressure evolution by fluid convection. In the limit that $T_i = T_e$, Eq. (32) reduces to

$$\gamma(\gamma^2+\omega_*^2)=\gamma_0^3. \tag{33}$$

Thus, for $\gamma \gg \omega_*$, $\gamma \cong \gamma_0$, the resistive MHD growth rate. For $\gamma < \omega_*$, $\gamma \cong \gamma_0^3/\omega_*^2$. Hence, a purely growing instability persists in the $\omega_* > \gamma$ limit. However, it should be noted that such persistence is a specialized consequence of the assumptions of $T_e = T_i$, zero temperature gradients, the neglect of order ω_D/ω corrections, and the electrostatic approximation. The inclusion of any of these effects yields an eigenmode with finite real frequency.

In the limit that the dispersion relation [Eq. (32)] applies, the asymptotic behavior of $\bar{\Phi}$ is given by $e^{-\lambda y^2}$, where

$$\lambda = \frac{1}{2}\left(-\frac{i\omega(\omega-\omega_{*i})}{\omega-\omega_{*e}}\frac{\hat{S}^2\eta k_\theta^2}{\omega_A^2}\right)^{1/2}. \tag{34}$$

Therefore, for such a solution to be valid, a necessary condition is $\mathrm{Re}(\lambda) > 0$. This condition is verified by all the solutions of Eq. (32) for any value of ω_{*i} and ω_{*e} (Fig. 1). Thus as γ passes from $\gamma > \omega_*$ to $\gamma < \omega_*$, the transition in growth rate expressions is a smooth one. In particular, although $\gamma \simeq \gamma_0^3/\omega_*^2$ appears directly proportional to η, the growth rate is still much faster than resistive diffusion. This is caused in part by the appearance of ρ^i as the perpendicular scale length, $\gamma = 2\eta n_i^2(T_e+T_i)^2q^2/[(B_0\rho_i V_i)^2 m_i n_i]$. However, in contrast to γ_0, which varies as $n^{2/3}$, $\gamma = \gamma_0^3/\omega_*^2$ is independent of the toroidal mode number. Thus, for increasing n, a finite diamagnetic frequency has a strong stabilizing influence relative to the MHD limit.

IV. NUMERICAL SOLUTION

Numerically we are interested in verifying the analytic solution of Sec. III and also in calculating the ω_* effects for equilibria reconstructed from experimental ISX-B data. To do so properly, we have to write the equations in a form consistent with a numerical solution of the Grad–Shafranov equation. The toroidal curvature and the field line bending term must be accurately represented without use of the aspect ratio expansions employed in deriving the approximate analytic solution. Also, numerically we use both a boundary value and initial value method. The initial value approach is easy to use and identifies the fastest growing solution. The boundary value approach requires a good guess of the solution but permits the tracking of eigenvalues in the complex plane. The initial value approach requires the time-dependent equations. These equations, whose equivalence to Eq. (21) will be demonstrated, are

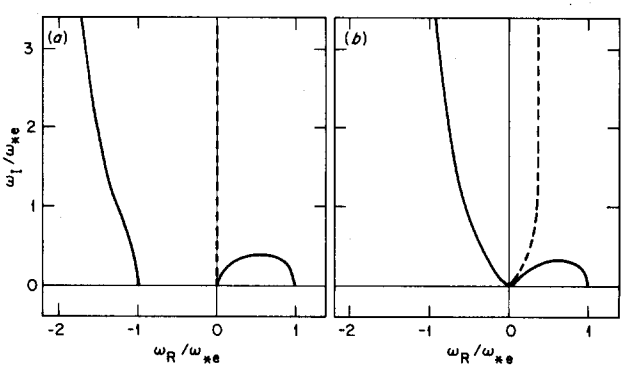

FIG. 1. Solid curves are the solution of $\mathrm{Re}(\lambda) = 0$ [cf. Eq. (34)] and broken curves are the solution of dispersion relation [Eq. (32)] for the cases $T_i = T_e$ [plot (a)] and $\omega_{*i} = 0$ [plot (b)]. Since in both cases the curves only intersect at $\omega_* = \infty$ the $\mathrm{Re}(\lambda) > 0$ for all ω_{*i} and ω_{*e} [N. B.: the case $\omega_{*e} = 0$ trivially verifies $\mathrm{Re}(\lambda) > 0$].

$$\frac{\partial A_{\|n}}{\partial t} = -i\omega_{*e} A_{\|n} - \eta k_\perp^2 A_{\|n} - \frac{1}{Rq}\frac{\partial \phi}{\partial y} + \frac{\omega_{*e}}{n_0}\frac{L_n}{k_\theta}\frac{I}{R}\frac{1}{Rq}\frac{\partial \tilde{n}}{\partial y}, \quad (35)$$

$$m_i n_0 \frac{\partial \Phi_n}{\partial t} = -ik_\theta \frac{B_0}{k_\perp^2}\frac{\hat{K}(y)}{R}\tilde{P} - \frac{IB_0^2}{Rk_\perp^2}\frac{1}{Rq} \times \frac{\partial}{\partial y}\left(\frac{k_\perp^2 A_{\|n}}{B_0}\right) - i\omega_{*i} m_i n_0 \Phi_n, \quad (36)$$

$$\frac{\partial \tilde{P}}{\partial t} = -ik_\theta \frac{R_0}{I}\frac{dP_0}{d\rho}\Phi_n, \quad (37)$$

$$\frac{\partial \tilde{n}}{\partial t} = -ik_\theta \frac{n_0}{L_n}\frac{R_0}{I}\Phi_n + \frac{1}{q_e B_0}\frac{I}{R}\frac{1}{Rq}\frac{\partial k_\perp^2 A_{\|n}}{\partial y}, \quad (38)$$

where P_0 is the equilibrium pressure and n_0 is the equilibrium density, $n_0 = n_e$.

Equation (35) is the generalized Ohm's law and corresponds to Eq. (18), where $J_{\|n} = -k_\perp^2 A_{\|n}$. Equation (36) is the momentum balance equation and corresponds to the $k_\perp \rho^i = 0$ limit of Eq. (15). Equation (37) is the convective evolution equation. Finally, Eq. (38) gives the evolution of the density; the $\nabla_\| J_\|$ will be neglected in accord with the argument given at the end of Sec. II.

Equations (35) through (38) may be recast in eigenvalue form by replacing the time derivatives by $-i\omega$. The resulting eigenvalue equation in the large aspect ratio limit is

$$\frac{\partial}{\partial y}\left(\frac{(\omega-\omega_{*e})k_\perp^2}{(\omega-\omega_{*e})+i\eta k_\perp^2}\frac{\partial \Phi_n}{\partial y}\right) + m_i n_0 \frac{R^2 q^2}{B_0^2} k_\perp^2 \omega(\omega-\omega_{*i})\Phi_n - \frac{Rq^2}{B_0^2} k_\theta^2 \frac{dP_0}{d\rho}\hat{K}(y)\Phi_n = 0, \quad (39)$$

where $\epsilon_p = [-R(dP_0/d\rho)/P_0]^{-1}$. This equation may be derived directly from Eq. (21) in the limit $k_\perp \rho^i = 0$ by taking $P_0 \equiv n_e(T_i + T_e)$.

Equation (39) is solved numerically using a library boundary value routine.[12] Equations (35) through (38) are solved as an initial value problem using a simple, explicit time advancement scheme. Detailed numerical tests have been made by comparing the results of these two methods of solution. Also, in the $\omega_* = 0$ limit comparisons have been made with a code[13] based on the equations of Ref. 3.

The numerical results of the eigenvalue equation, Eq. (39), have been compared with the analytic dispersion relation, Eq. (32), for several equilibria and values of the parameters $S^{-1}n^2$, ω_{*e}, and ω_{*i}, where the dimensionless parameter S is $S = a^2 V_A/[R\eta(0)]$. An example is shown in Fig. 2 for an equilibrium matching ISX-B experimental results with $\beta_p = 1.29$. This equilibrium was calculated in the manner described in Ref. 14. Figure 2 shows how the linear growth rate varies as a function of ω_* for the case $T_e = T_i$, and $S^{-1}n^2 = 10^{-5}$. For the purpose of these comparisons, ω_* is taken as an independent parameter. Also plotted in the same figure is the root of the dispersion relation, Eq. (33). For these parameters good agreement is displayed with the analytic results. Good agreement is also found for other ratios of T_e/T_i, in particular in the limits $T_i = 0$ and $T_e = 0$. Figure 3 shows these limits ($\omega_{*i} = 0$ and $\omega_{*e} = 0$) for the same parameters as Fig. 2.

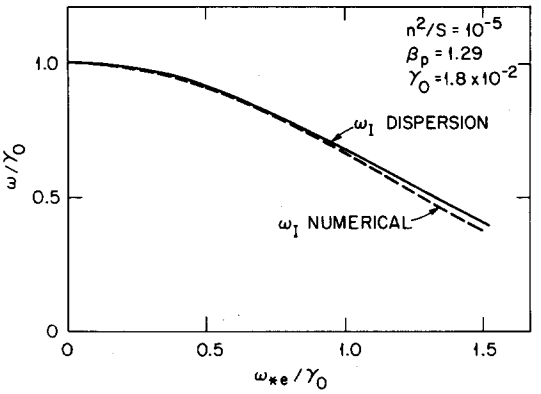

FIG. 2. Growth rates as a function of ω_{*e} for the case $T_e = T_i, \beta_p = 1.29$, $\rho = 0.5$, and $n^2/S = 10^{-5}$.

Here, the regime of primary interest to ISX-B is that of high β_p. In this regime, the model for anomalous electron heat conduction described in Ref. 5 becomes relevant. To study this regime an equilibrium with $\beta_p = 2.0$ and q varying between 0.9 at the magnetic axis and 7.0 at the plasma edge is considered. Figure 4 shows the comparison with the analytic dispersion relation, Eq. (33), for the case $T_i = T_e$, $S = 10^6$, and $n = 15$. Results are shown for two flux surfaces $\rho = 0.5$ and $\rho = 0.7$. Qualitative agreement is again displayed with the analytic solution. However, in this case the quantitative agreement is not as good. This is mainly because of the high shear of this equilibrium, $\hat{S} = 1.9$ at $\rho = 0.7$. For such high shear equilibria the two-scale-lengths expansion made in de-

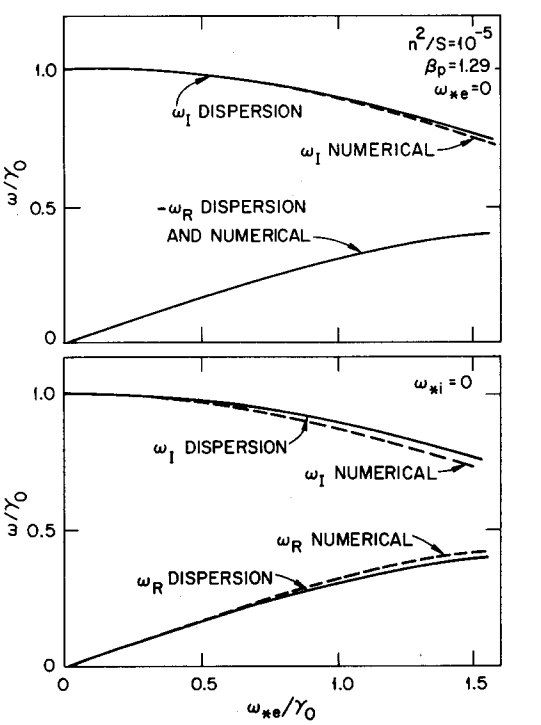

FIG. 3. Growth rates as a function of ω_* for the same parameters as Fig. 2 but with $\omega_{*e} = 0$ (upper plot) and $\omega_{*i} = 0$ (lower plot).

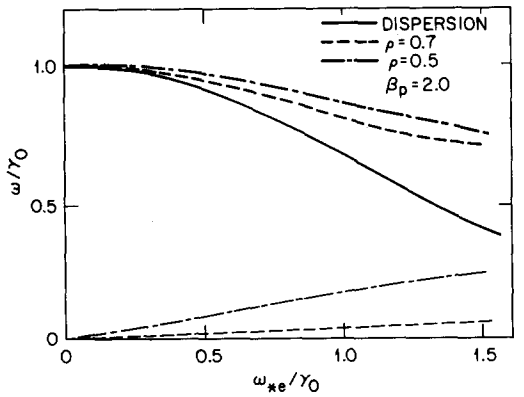

FIG. 4. Growth rates as a function of ω_* for the case $T_e = T_i$, $\beta_p = 2.0$, $\rho = 0.5$ and 0.7, $S = 10^6$, and $n = 15$.

riving the analytic dispersion relation breaks down.

The analytic solution of the dispersion relation, Eq. (33), has been found numerically for all equilibria studied. However, in the $\omega_* \gtrsim \gamma_0$ regime, this solution does not always correspond to the fastest-growing mode. In certain regions of parameter space, the numerical solution of the eigenvalue problem shows a much more complicated picture than the analytic dispersion relation. There are eigenvalues with imaginary parts that do not decrease with ω_* as fast as predicted by the analytic solution; some eigenvalues show increased instability with ω_*, and some solutions bifurcate at a given value of ω_*. Figure 5 illustrates these problems by showing the ω_* dependence of several roots of the eigenvalue problem for the same equilibrium as Fig. 2 but with $n^2 S^{-1} = 4 \times 10^{-4}$.

V. NONLINEAR SATURATION AND ANOMALOUS ELECTRON THERMAL CONDUCTIVITY

In this section the nonlinear saturation of kinetic resistive ballooning modes is discussed and the resulting anomalous electron thermal conductivity is calculated. The nonlinear theory of resistive ballooning modes is developed by using renormalized ion and electron kinetic equations and the procedure of Sec. II to derive a nonlinear (amplitude-dependent) ballooning mode dispersion relation. The saturation amplitude is then computed from the condition $\gamma = 0$. Following Ref. 5, the anomalous electron thermal conductivity is estimated using the result of the nonlinear analysis.

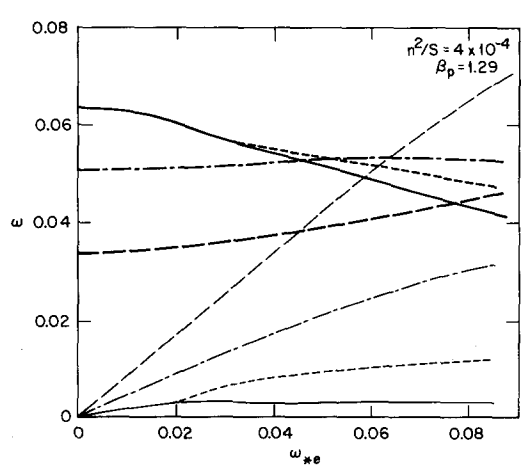

FIG. 5. Real (light curves) and imaginary (thick curves) growth rates as a function of ω_* for the same equilibrium as Fig. 2 but with $n^2/S = 4 \times 10^{-4}$. The finite ω_* behavior of a few of the many unstable roots is shown, with the corresponding real and imaginary parts depicted by the same type of curve.

The procedure followed in this section is to construct the continuity equation, $\nabla \cdot \mathbf{J} = 0$, by subtracting the density moments of the renormalized gyrokinetic equations. The current moment of the renormalized electron drift kinetic equation is then used to derive Ohm's law. The electrostatic approximation is assumed throughout the discussion of nonlinear saturation. This approximation is consistent with the resistive instability condition that dissipation weakens the stabilizing influence of field line bending ($\eta k_\perp^2 > \gamma$). It follows that $E_K > E_M$, where

$$E_K = \int dy \sum_n k_\perp^2(y) \langle \Phi(y)^2 \rangle_n, \tag{40}$$

$$E_M = \int dy \sum_n k_\perp^2(y) \langle A_\parallel(y)^2 \rangle_n \tag{41}$$

are the electrostatic and magnetic energies of the fluctuations. Therefore, the electrostatic approximation and the condition $\lambda_{\text{mfp}} < Rq$ imply that the principal electron nonlinearity is that associated with $c\mathbf{E} \times \mathbf{B}_0 / B_0^2$ convection. Hence the electrostatic approximation ensures that the time scales for the nonlinear evolution of electron density and parallel current are comparable to the nonlinear ion (electrostatic) time scales, thus maintaining $\nabla \cdot \mathbf{J} = 0$. It is important to note that these considerations and constraints apply to electron density and current but not to electron temperature.

The nonlinear ion gyrokinetic equation[15] in toroidal geometry is

$$-i(\omega - \omega_{Di}) g_n^i + \frac{V_\parallel}{Rq} \frac{\partial g_n^i}{\partial y} + N_n^i(y) = -i(|e|/T_i)(\omega - \omega_{*i}) J_0(k_\perp \rho^i) \Phi_n \langle f^i \rangle, \tag{42}$$

with

$$N_n^i(y) = \sum_{n'} \sum_{m'} C(n,n',m') [J_0(k'_\perp \rho^i) \Phi_{-n'}] \, g_{n+n'}^i(y), \tag{43}$$

$$C(n,n',m') = k_\theta \, k'_\theta \, \hat{S}(2\pi m') e^{-2\pi i m' n' q(\rho)}. \tag{44}$$

Inductive effects, which are unimportant for ions, have been neglected. Here $N_n^i(y)$ is the nonlinear term contribution evaluated at y. Quantities enclosed in square brackets are to be evaluated at $y + 2\pi m$. Contributions from $y + 2\pi m$ introduce additional phase factors into $C(n,n',m')$. As such phase factors tend to produce cancellation when m is summed, only the $m = 0$ piece is retained. In order to simplify the calculation, the additional assumptions of $k_\perp^2 (\rho^i)^2 < 1$, $\omega_{Di}/\omega \ll 1$ and $y_0 = 0$, where y_0 is the ballooning eikonal phase, have been invoked. The third assumption implies that the results of this calculation constitute a lower bound on the nonlinear interaction.

Following Ref. 16, the renormalized ion nonlinearity is

$$N_n^i(y) = \sum_{n'} \sum_{m'} C(m,n',m') [J_0(k'_\perp \rho^i) \Phi_{-n'}] \, g_{n+n'}^{i(2)}, \tag{45}$$

where

$$(L^{i}_{n+n'})^{-1} g^{i(2)}_{n+n'} = \sum_{m''} C^{*}(n,n',m'') \times \{ [J_0(k'_\perp \rho^i)\Phi_{n'}]\, g^{i}_{n} - [\, g^{i}_{n'}]J_0(k_\perp \rho^i)\Phi_n \}, \quad (46)$$

with

$$(L^{i}_{n+n'})^{-1} = i(\omega'' - \omega''_{Di} + id_{n''}) + \frac{V_\parallel}{Rq}\frac{\partial}{\partial y}. \quad (47)$$

Here $\omega'' = \omega + \omega'$, $\omega''_{Di} = \omega_{Di} + \omega'_{Di}$, and $d_{n''}$ is a propagator broadening factor that accounts for ion scattering by heat fluctuations. It follows directly that

$$N^{i}_{n}(y) = d_n\, g^{i}_{n} - (|e|/T_i)\langle f^{i}\rangle b_n\, J_0(k_\perp \rho^i)\Phi_n, \quad (48)$$

where

$$d_n = \sum_{n'}\sum_{m'} |C(n,n',m')|^2 \times [J_0^2(k'_\perp \rho^i)\langle \Phi^2\rangle_{n'}]L^{i}_{n+n'}, \quad (49)$$

$$b_n = \sum_{n'}\sum_{m'} |C(n,n',m')|^2 \times [J_0(k'_\perp \rho^i)\langle \Phi h^{i}\rangle_{n'}]L^{i}_{n+n'}, \quad (50)$$

and h^{i}_{n} is defined such that $g^{i}_{n} = |e|\langle f^{i}\rangle h^{i}_{n}/T_i$.

Contributions from $m' \neq m''$ introduce phase factors that result in cancellation. As $\tilde{\Phi} \ll \bar{\Phi}$ [Eq. (26)] and because the mode is extended in y, $L_{n+n'} \cong -i(\omega'' - \omega''_{Di} + id_{n''})$. Thus the renormalized ion kinetic equation is

$$-i(\omega - \omega_{Di} + id_n)g^{i}_{n} + \frac{V_\parallel}{Rq}\frac{\partial g^{i}_{n}}{\partial y} = (i|e|/T_i)\langle f^{i}\rangle(\omega - \omega_{*i} + ib_n)J_0(k_\perp \rho^i)\Phi_n, \quad (51)$$

and the nonlinear ion response is

$$g^{i}_{n} = \frac{|e|}{T_i}\frac{\omega - \omega_{*i} + ib_n}{\omega - \omega_{Di} + id_n}\Phi_n\, J_0(k_\perp \rho^i). \quad (52)$$

Note that Eq. (52) also gives $h^{i}_{n'}$ in the expression for b_n. The physical interpretation of this renormalization procedure is that in the presence of a broad turbulent spectrum, ion Compton scattering[17,18] by nonlinearly drive fluctuations, denoted by n'', results in the modification of the ion response to a particular test mode. Alternatively, it may be said that a test mode n couples to the turbulent test mode spectrum $\langle \Phi^2\rangle_{n'}$ through the nonlinearity driven beat fluctuations n''. Ion Compton scattering by resistive ballooning modes differs from the more familiar case of drift wave turbulence in two important aspects. First, in contrast to the drift wave case, the electron response is hydrodynamic, not adiabatic. Hence induced potential effects (associated with $\Phi^{(2)}_{n''}$), which cancel $g^{(2)}_{n''}$ to lowest order in $(k_\perp \rho^i)^2$ for adiabatic electron response and quasineutrality, are much less important here and are thus neglected. Second, for a saturated state that has evolved from a spectrum of purely growing modes, $\omega = 0$ and $d_n \gg \omega_{Di}$. Therefore, d_n and b_n are similar to turbulent eddy viscosities, which achieve saturation by balancing the linear driving forces. This is very different from the drift wave case, where d_n and b_n admit a nonlinear dissipation through the beat fluctuation resonances of d_n. This is caused by the fact that ballooning mode growth is a consequence of a balance of forces, while drift instability is a consequence of the introduction of inverse dissipation into a marginally stable oscillation.

The renormalized electron drift kinetic equation can be constructed in a similar fashion. The nonlinear electron kinetic equation is

$$-i(\omega - \omega_{De})g^{e}_{n} + \frac{V_\parallel}{Rq}\frac{\partial g^{e}_{n}}{\partial y} + \mathscr{C} g^{e}_{n} + N^{e}_{n}(y) = i(|e|/T_e)(\omega - \omega_{*e})[\Phi_n - (V_\parallel/c)A_{\parallel n}]\langle f^{e}\rangle, \quad (53)$$

with the nonlinear term N^{e}_{n} given by

$$N^{e}_{n}(y) = \sum_{n'}\sum_{m'} C(n,n',m') \times \{ [\Phi_{-n'} - (V_\parallel/c)A_{\parallel -n'}]\}g^{e}_{n+n'}, \quad (54)$$

where the same conventions as the ion case are used. The renormalized electron nonlinearity is

$$N^{e}_{n}(y) = \sum_{n'}\sum_{m'} C(n,n',m) \times \{ [\Phi_{-n'} - (V_\parallel/c)A_{\parallel -n'}]\}g^{e(2)}_{n+n'}, \quad (55)$$

with $g^{e(2)}_{n+n'}$ given by

$$(L^{e}_{n+n'})^{-1} g^{e(2)}_{n+n'} = \sum_{m''} C^{*}(n,n',m'') \times (\{ [\Phi_{n'} - (V_\parallel/c)A_{\parallel n'}]\}g^{e}_{n} - (g^{e}_{n'})[\Phi_n - (V_\parallel/c)A_{\parallel n}]), \quad (56)$$

and the operator $L^{e}_{n+n'}$ defined by

$$(L^{e}_{n+n'})^{-1} = -i(\omega'' - \bar{\omega}''_{De} + iD_{n''}) + \frac{V_\parallel}{Rq}\frac{\partial}{\partial y} + \mathscr{C}. \quad (57)$$

In the short-mean-free path limit where $|\mathscr{C}| > \omega_{Te}$, Eq. (56) may easily be solved to yield

$$g^{e(2)}_{n+n'} = L^{e}_{n+n'} \sum_{m''} C^{*}(n,n',m'') \times \{ [\Phi_{n'}]\, \bar{g}^{e}_{n} - [\, \bar{g}^{e}_{n'}]\Phi_n \}\langle f^{e}\rangle, \quad (58)$$

$(L^{e}_{n+n'})^{-1} = -i(\omega'' - \bar{\omega}''_{De} + iD_{n''})$.

Note that Eq. (58) is clearly consistent with the electrostatic approximation ($E_K \gg E_M$). Neglecting the insignificant inductive-electrostatic cross terms, it follows that

$$N^{e}_{n}(y) = D_n\, \bar{g}^{e}_{n}\langle f^{e}\rangle - (|e|/T_e)\langle f^{e}\rangle B_n \Phi_n, \quad (59)$$

where

$$D_n = \sum_{n'}\sum_{m'} |C(n,n',m')|^2 [\langle \Phi^2\rangle_{n'}]L^{e}_{n+n'}, \quad (60)$$

$$B_n = \sum_{n'}\sum_{m'} |C(n,n',m')|^2 [\langle \Phi \bar{h}^{e}\rangle_{n'}]L^{e}_{n+n'}, \quad (61)$$

with $\bar{h}^{e}$ defined such that $\bar{g}^{e} = |e|\bar{h}^{e}/T_e$. The renormalized electron kinetic equation is thus

$$-i(\omega - \omega_{De})g^{e}_{n} + \frac{V_\parallel}{Rq}\frac{\partial g^{e}_{n}}{\partial y} + D_n\, \bar{g}^{e}_{n}\langle f^{e}\rangle + \mathscr{C} g^{e}_{n} = \frac{i|e|}{T_e}\left[(\omega - \omega_{*e})\left(\Phi_n - \frac{V_\parallel}{c}A_{\parallel n}\right) - iB_n\Phi_n\right]\langle f^{e}\rangle. \quad (62)$$

The electron response is

$$g_n^e = -\frac{|e|}{T_e}\frac{\omega-\omega_{*e}-iB_n}{\omega-\bar{\omega}_{De}+iD_n}\langle f^e\rangle\Phi_n. \tag{63}$$

The renormalized macroscopic equations may now be constructed using the procedure of Sec. II. In the limit where $(k_\perp\rho^i)^2<1$ and $\omega_{Di}/\omega\ll 1$, subtracting the density moment of Eq. (62) from the corresponding moment of Eq. (51) and using Eqs. (52) and (63) to compute the curvature drift terms yields

$$\begin{aligned} i\left(\frac{a_eV_A}{c}\right)^2\frac{1}{Rq}\frac{\partial J_{\|n}}{\partial y} &= -(k_\perp a_e)^2(\omega-\omega_{*i}+ib_n)\Phi_n \\ &\quad+\left(\frac{\bar{\omega}_{Di}(-\omega_{*i}+ib_n)}{\omega+iD_n}-\frac{\tau\bar{\omega}_{De}(\omega_{*e}+iB_n)}{\omega+iD_n}\right)\Phi_n. \end{aligned} \tag{64}$$

Here the limit $(k_\perp\rho^i)^2<1$ allows the approximation $d_n\cong D_n$. Similarly, constructing the $V_\|$ moment of Eq. (62) using the result of Eq. (63) to calculate $P_{\|n'}$ yields the renormalized Ohm's law

$$\begin{aligned} \left(\frac{c^2\nu_{ei}}{\omega_{pe}^2}k_\perp^2-i(\omega-\omega_{*e})\right)\frac{A_{\|n}}{c} &= -\frac{\omega-\omega_{*e}-iB_n}{\omega+iD_n}\frac{1}{Rq}\frac{\partial\Phi}{\partial y}. \end{aligned} \tag{65}$$

Electrostatic effects only appear in Eq. (65). The significance of this approximation and the consequences of retaining magnetic effects will be discussed in a forthcoming publication.

Combining Eqs. (64) and (65) gives the nonlinear resistive ballooning equation

$$\begin{aligned} &i\omega_A^2\left(\frac{\omega-\omega_{*e}-iB_n}{\omega+iD_n}\right)\frac{\partial}{\partial y}\left(\frac{(k_\perp a_e)^2}{\eta k_\perp^2-i(\omega-\omega_{*e})}\frac{\partial\Phi_n}{\partial y}\right) \\ &\quad-(k_\perp a_e)^2(\omega-\omega_{*i}+ib_n)\Phi_n \\ &\quad-\left(\frac{(\bar{\omega}_{Di}\omega_{*i}+\tau\bar{\omega}_{De}\omega_{*e})}{\omega+iD_n}\right. \\ &\quad\left.-i\frac{(\bar{\omega}_{Di}b_n-\tau\bar{\omega}_{De}B_n)}{\omega+iD_n}\right)\Phi_n=0. \end{aligned} \tag{66}$$

It should be noted that the renormalized equations are consistent with constraints imposed by the basic nonlinear equations. Equation (64) is the renormalized continuity equation, obtained by subtracting the density moments of the renormalized kinetic equations. Subtracting the density moments of the electrostatic nonlinearities of the kinetic equations yields F_E, where

$$F_E=\frac{C}{B_0}\left(\int d^3V_i\,J_0(k_\perp\rho^i)(\langle\nabla\Phi\rangle_\phi\times\hat{n}\cdot\nabla g^i)_k - \int dV_\|\,[(\nabla\Phi\times\hat{n})\times\nabla g^e]_k\right). \tag{67}$$

The angle brackets $\langle\ \rangle_\phi$ indicate a gyrophase average. In the limit $(k_\perp\rho^i)^2<1$, $\omega_D/\omega<1$, and $k_\|\to 0$, that is, $\partial\Phi/\partial y\to 0$, F_E becomes

$$F_E=(C/B_0)(\nabla\Phi\times\hat{n}\cdot\nabla[\rho_q^i-\rho_q^e])_k,$$

where ρ_q^i and ρ_q^e are the nonadiabatic ion and electron charge densities. It follows from quasineutrality that F_E vanishes to lowest order in $k_\perp^2(\rho^i)^2$, ω_D/ω, and $k_\|$. It is easily verified that the D_n, b_n, and B_n terms in Eq. (64) appear in a manner consistent with this property of the basic equations. Note that the approximation $d_n=D_n$, a consequence of $(k_\perp\rho^i)^2<1$, facilitated casting the continuity equation in the form of Eq. (64). Finally, it should be mentioned that the constraint discussed here is different from that discussed in Ref. 14, which is also satisfied by the renormalized equations.

In order to make contact with the discussion of linear theory, the nonlinear saturation for the case $T_i=T_e$, which results linearly in a purely growing mode, is now discussed. In this case $\omega=i\gamma_n$ and $\omega'=i\gamma_{n'}$ and

$$(L_{n+n'}^{e,i})^{-1}=(\gamma_n+\gamma_n+iD_{n'}), \tag{68}$$

$$b_n=\sum_n\sum_{m'}|C(n,n',m')|^2[\langle\Phi^2\rangle_{n'}]\times[(\gamma_{n'}+i\omega_{*i}+b_{n'})/(\gamma_{n'}+D_{n'})]L_{n'}^i, \tag{69}$$

$$B_n=\sum_n\sum_{m'}|C(n,n',m')|^2[\langle\Phi^2\rangle_{n'}]\times[(\gamma_{n'}-i\omega_{*e}-B_{n'})/(\gamma_{n'}+D_{n'})]L_{n'}^e. \tag{70}$$

The difference in sign between b_n and B_n is caused by the difference in sign between the ion and electron nonadiabatic responses. For $\langle\Phi^2\rangle_{-n}=\langle\Phi^2\rangle_n$, it follows that the ω_* contributions to b_n and B_n vanish by antisymmetry. Then for $b_{n'}=D_{n'}$, $B_{n'}=-D_{n'}$, and thus $b_n=D_n$ and $B_n=-D_n$, which constitutes a consistent solution to the recursive Eqs. (69) and (70). Hence, Eq. (66) reduces to

$$\begin{aligned} &\omega_A^2(\gamma+D_n+i\omega_*)\frac{\partial}{\partial y}\left(\frac{k_\perp^2}{\eta k_\perp^2+\gamma+i\omega_*}\frac{\partial\Phi_n}{\partial y}\right) \\ &\quad-[k_\perp^2(\gamma+D_n-i\omega_*)(\gamma+D_n) \\ &\quad-2k_\theta^2\gamma_I^2\hat{K}(y)]\Phi_n=0. \end{aligned} \tag{71}$$

The two-scale averaging procedure discussed in Sec. III can now be applied to Eq. (71). Upon invoking the electrostatic approximation for $\bar{\Phi}_n$, the resulting dispersion relation is

$$(\gamma+D_n)((\gamma+D_n)^2+\omega_*^2)=\gamma_0^3. \tag{72}$$

Setting $\gamma=0$ yields

$$D_n(D_n^2+\omega_*^2)=\gamma_0^3, \tag{73}$$

where

$$D_n=\frac{c^2k_\theta^2\hat{S}^2}{B_0^2}\sum_{n'}\sum_m k_\theta'^2\langle\Phi^2(y+2\pi m)\rangle_n L_{n+n'}(2\pi m)^2, \tag{74}$$

and

$$L_{n+n'}=(\gamma_n+\gamma_{n'}+D_{n'})^{-1}. \tag{75}$$

Thus for $D_n>\omega_*$, $D_n=\gamma_0$, which recovers the resistive MHD result.[5] For $\omega_*>D_n=\gamma_0^3/\omega_*^2$. The extent of the mode W_n in y is given by

$$W_n=[4\omega_A^2/(D_n\eta k_\theta^2\hat{S}^2)]^{1/4}. \tag{76}$$

It is illuminating to note that $D_n=k_\theta^2\hat{D}_n$, where $\hat{D}_n$ is non-Markovian (n dependent) and analogous to a diffusion

coefficient. Indeed, in the limit $n \to 0$, $\hat{D}$ is the $c\mathbf{E}\times\mathbf{B}_0/B_0^2$ diffusion coefficient. Hence, the physical content of the saturation condition is that the turbulence generates random convection sufficient to balance the driving forces at $\gamma = 0$. Alternatively, when turbulent convection leads to a decorrelation time τ_{cn} ($\tau_{cn}^{-1} = D_n$ here) such that $\tau_{cn}^{-1} = \gamma_{cn}$, a particle or pressure element responding to driving forces is decorrelated at a rate equal to the rate of growth caused by driving forces. Hence, the instability cannot grow and saturation occurs. The decorrelation results from scattering a density or pressure element over a poloidal subharmonic width Δy, $\Delta y = (k_\theta \hat{S})^{-1} W_n$, in a growth time. Finally, from the structure of the linear dispersion relation, it is apparent that balance with driving forces requires diffusion of ion density (inertia), electron and ion pressure, and electron parallel pressure. These correspond to D_n terms appearing in the inertia, curvature drive, and line bending (from Ohm's law) pieces of Eq. (71), respectively.

In general, kinetic resistive ballooning instabilities develop a finite frequency and are not purely growing. In that case, several new nonlinear phenomena may appear. First, nonlinear dissipation may enter through the broadened beat wave-particle resonances in d_n, D_n, b_n, and B_n. Second, b_n and B_n will in general be complex. Hence, b_n and B_n will introduce nonlinear frequency shifts as well as eddy viscosity effects. This second point is especially important, since the diffusion at saturation would then be determined by linear frequency effects, reduced or enhanced by nonlinear frequency shifts. Hence the ultimate answer to the question "What is the impact of kinetic effects on ballooning mode turbulence?" probably lies in the nonlinear dynamics.

It should be added that there are many aspects of the nonlinear theory that must be considered. Here the parameter scalings of the saturation level and the electron heat conduction coefficient χ_e are of primary interest. However, to understand the structure and evolution of the wavenumber and frequency spectrum, a theory of the two-point correlation is required. This will be considered in a future publication.

In Ref. 5 an estimate of the anomalous electron thermal conductivity was obtained by using Ohm's law and the electrostatic energy at saturation to calculate D_M, the stochastic magnetic field line diffusion coefficient, and thus χ_e, $\chi_e \cong (3/2) V_{Te} D_M$. The electrostatic energy at saturation was obtained from the saturation condition $D_n = \gamma$. It is important to note that D_M was calculated for the relevant regime of strong turbulence, $D_M \sim |\delta B / B_0|$.

Following Ref. 5, D_M is given by

$$D_M \approx \left(\frac{\Sigma_{n'} \Sigma_{m'} |A_{\|n'}(y + 2\pi m')|}{(B_0^2 \hat{S}^2 W_n^2)} \right)^{1/2}, \tag{77}$$

where, for finite diamagnetic frequency and $\eta k_\perp^2 > |\omega - \omega_{*e}|$,

$$\frac{A_{\|n}}{c} = -\frac{D_n + i\omega_{*e}}{D_n} \frac{1}{\eta k_\perp^2} \frac{1}{Rq} \frac{\partial \Phi_n}{\partial y}. \tag{78}$$

The saturation condition Eqs. (73) and (74) implies

$$\overline{(c^2/B_0^2) k_\theta^2 \langle \Phi^2 \rangle_n} \approx \overline{D_n^2 \Delta_n^2}, \tag{79}$$

where the elevated bar indicates the spectrum average and $\Delta_n = (k_\theta \hat{S} W_n)^{-1}$. Equation (79) determines the electrostatic perturbation at saturation. Substituting Eq. (78) into Eq. (77) and using Eq. (79) yields

$$D_M \approx \frac{\eta}{Rq} \sum_n \left(\frac{nq\hat{S}W_n}{\rho} \right)^{-4} \left| \frac{D_n + i\omega_*}{D_n} \right| \frac{D_n}{W_n} F(y). \tag{80}$$

Here $F(y)$ is a dimensionless spectrum structure function. Straightforward algebra then yields

$$\chi_e = \chi_e^{(0)} (1 + |\omega_*/\gamma|^2)^{-1/4}, \tag{81}$$

where $\chi_e^{(0)}$ is the electron heat diffusion coefficient derived in Ref. 5 for the resistive MHD modes. For $\overline{\omega_*/\gamma} \ll 1$, we have

$$\chi_e = \chi_e^{(0)} \propto \beta_p^{3/2} T_e^{-1}, \tag{82}$$

and for $\overline{\omega_*/\gamma} \gg 1$,

$$\chi_e = \chi_e^{(0)} \overline{(\omega_*/\gamma_0)}^{-3/2} \propto \beta_p^{5/2} T_e^{-13/4}. \tag{83}$$

Obviously, if appreciable populations of $\gamma_0 > \omega_*$ and $\gamma_0 < \omega_*$ modes are present, then a weighted spectrum average must be performed. Finally, note that the basic structure of strong β_p dependence and inverse T_e dependence persists in the large ω_* regime.

It is interesting to observe that the factor $|(D_n + i\omega_{*e})/D_n|$ in Eq. (80) indicates that when $\omega_* > D_M$, the level of electromagnetic fluctuations increases relative to that of electrostatic fluctuations. This indicates that while inclusion of diamagnetic effects may result in a growth rate reduction relative to the predictions of magnetohydrodynamics, it may also result in an increase in other effects contributing to heat transport. This is an example of the dangers inherent in the practice of assuming that anomalous transport behavior directly tracks the behavior of linear growth rates.

VI. CONCLUSIONS

The linear and nonlinear kinetic theory of resistive ballooning modes has been presented. It has been shown that the inclusion of kinetic effects associated with finite Larmor radius, diamagnetic frequency, and drift frequency in general modifies the linear stability of resistive ballooning modes. However, for equilibria associated with high β_p ISX-B discharges, these effects do not fundamentally change the linear stability spectrum in the range of relevant toroidal mode numbers ($n \lesssim 50$). Therefore, these instabilities are expected to be present in the experiment.

The nonlinear kinetic theory modifies the predicted value of the electron heat diffusivity derived in the reduced MHD model.[5] However, the modification is quantitatively small. Although the ω_* effects reduce the linear growth of the instability and, thus, the saturated level of the electrostatic fluctuations; the level of the electromagnetic fluctuations increases with ω_* relative to that of electrostatic fluctuations. Therefore, the overall ω_* effect on the electron heat transport is weaker than what naively would be expected.

ACKNOWLEDGMENTS

The authors are grateful to M. N. Rosenbluth for many helpful conversations. Stimulating criticism from A. H.

Glasser and encouragement from W. M. Tang are acknowledged. We would also like to thank L. A. Charlton and J. A. Holmes for providing us with the equilibria used in the numerical calculations.

This research was sponsored by the Office of Fusion Energy, U. S. Department of Energy, under Contract No. W-7405-eng-26 with the Union Carbide Corporation and under Contract No. DOE/ET/53088 with the Institute for Fusion Studies.

[1]H. P. Furth, J. Killeen, M. N. Rosenbluth, and B. Coppi, in *Proceedings of the Second International Conference on Plasma Physics and Controlled Nuclear Fusion Research* (IAEA, Vienna, 1966), Vol. I, p. 103.
[2]M. S. Chance, R. L. Dewar, E. A. Frieman, A. H. Glasser, J. M. Greene, R. C. Grimm, S. C. Jardin, J. L. Johnson, J. Manickam, M. Okabayashi, and A. M. M. Todd, in *Proceedings of the Seventh International Conference on Plasma Physics and Controlled Nuclear Fusion Research* (IAEA, Vienna, 1979), Vol. I, p. 677.
[3]G. Bateman and D. B. Nelson, Phys. Rev. Lett. **41**, 1809 (1978).
[4]H. R. Strauss, Phys. Fluids **24**, 2004 (1981).
[5]B. A. Carreras, P. H. Diamond, M. Murakami, J. L. Dunlap, J. D. Bell, H. R. Hicks, J. A. Holmes, E. A. Lazarus, V. K. Paré, P. Similon, C. E. Thomas, and R. M. Wieland, Phys. Rev. Lett. **50**, 503 (1983).
[6]T. C. Hender, B. A. Carreras, W. A. Cooper, J. A. Holmes, P. H. Diamond, and P. L. Similon, University of Texas at Austin, Institute for Fusion Studies Report No. IFS 108, 1983.
[7]T. M. Antonsen and B. Lane, Phys. Fluids, **23**, 1205 (1980).
[8]P. J. Catto, W. M. Tang, and D. E. Baldwin, Plasma Phys. **23**, 639 (1981).
[9]W. M. Tang, J. W. Connor, and R. J. Hastie, Nucl. Fusion **20**, 1439 (1980).
[10]S. I. Braginskii, in *Reviews of Plasma Physics*, edited by M. A. Leontovich (Consultants Bureau, New York, 1965), Vol. I, p. 205.
[11]D. Biskamp, Nucl. Fusion **18**, 1059 (1978).
[12]M. E. Lord, M. R. Scott, and H. A. Watts, in *Applied Nonlinear Analysis* (Academic, New York, 1979), pp. 635–656.
[13]W. A. Cooper (private communication).
[14]L. A. Charlton, G. H. Neilson, and R. M. Wieland, Phys. Fluids (to be published).
[15]E. A. Frieman and L. Chen, Phys. Fluids **25**, 502 (1982).
[16]T. H. Dupree and D. J. Tetreault, Phys. Fluids **21**, 425 (1978).
[17]P. H. Diamond and M. N. Rosenbluth, Phys. Fluids (to be published).
[18]P. Similon and P. H. Diamond, Phys. Fluids **27**, 916 (1984).